



Impact of Vibrations on the Physical and Mechanical Properties of Concrete: Case Study of Constructions in the City of Douala Cameroon

Andre Abanda¹, Fabien Kenmogne^{2,*}, Martial Nde Ngnihamy³, Blaise Ngwem Bayiha², Ekoum Ewandjo Nkoue¹, Roger Eno¹, Etienne Marc Ndtoungou², Willy Arnold Donda Fonchou², Emmanuel Yamb Bell²

¹Department of Civil Engineering, National Advanced Polytechnical School, University of Douala, Douala, Cameroon

²Department of Civil Engineering, Advanced Teachers Training College of the Technical Education, University of Douala, Douala, Cameroon

³Department of Civil Engineering, National Advanced School of Public Works, Yaoundé, Cameroon

Email address:

kenfabien@yahoo.fr (Fabien Kenmogne)

*Corresponding author

To cite this article:

Andre Abanda, Fabien Kenmogne, Martial Nde Ngnihamy, Blaise Ngwem Bayiha, Ekoum Ewandjo Nkoue et al. (2024). Impact of Vibrations on the Physical and Mechanical Properties of Concrete: Case Study of Constructions in the City of Douala Cameroon. *Journal of Civil, Construction and Environmental Engineering*, 9(1), 9-26. <https://doi.org/10.11648/jccee.20240901.12>

Received: January 6, 2024; **Accepted:** January 20, 2024; **Published:** February 1, 2024

Abstract: In the field of construction, concrete is the most consumed material. Despite the arrival on the market of fluid concretes such as self-compacting concretes, ordinary concretes still represent the most used on construction sites today. In order to finalize the filling of the formwork and achieve the expected performance, these concretes are vibrated occasionally using a vibrating needle. In this work, the impact of vibrations on the physical and mechanical properties of concrete in the city of Douala Cameroon is investigated, taking into account the recent progress in the field of use and improvement of concrete material. Firstly, the concrete material is analyzed by looking at its use, its formulations, its physical-mechanical characteristics and its behavior with regard to the environment. Then the mechanical characteristics representative of available vibration equipment is identified. Using the formulations obtained, the fluidity and consistency ranges over which vibration of the material is necessary is identified. A simple analytical model to predict the action diameter of the vibrator is then developed and compared to the experimental results found. Finally, a minimum vibration time value necessary for compaction of the material is quantified as well as a minimum vibration time value necessary for improving the physical and mechanical quality of the facing after vibration and setting of the concrete.

Keywords: Self Compacting Concrete, Threshold Fluid, Rheology, Vibration Time, Viscosity

1. Introduction

Fresh concrete has the appearance of liquid stone, and the aggregates that compose it are carried by a viscous paste which flows under the action of effort [1]. Its manufacturing requires highly available natural resources, sand and gravel distributed across the entire planet and inexpensive [2, 3]. In addition, its easy handling ensures that elements of complex shapes can be obtained and requires unskilled labor. In its hardened state, concrete provides significant mechanical

strength and allows the construction of imposing structures such as large viaducts or immense skyscrapers built at the start of the 21st century [4]. Thus, all its advantages give it the status of the most consumed material in the world. National and international recommendations for the implementation of concrete suggest the application of vibration, internal or external, to implement it [5]. From a macroscopic point of view, it locally liquefies the material, promotes its flow through the metal reinforcements and helps its compaction [6]. Traditionally, on construction sites,

internal vibration by vibrating needle, also called pervibration, constitutes the most used technique [7]. Although knowledge of the rheology of cementitious materials has progressed significantly in recent years, the arrival on the markets of self-compacting fluid concretes has also slowed down any research efforts on vibration [8]. The new knowledge currently have on rheology, interactions between particles and flow simulation allows today to return to this subject in order to obtain a better understanding. In this context, based on current existing literature and recent developments in concrete formulations and implementation, it is necessary to provide elements of answers to the following questions: Does concrete that has been vibrated for a long time has its mechanical properties improved and its porosity reduced? Does concrete that has been vibrated for a long time increase its adhesion to reinforcement and its density? What about the effect of Douala sand on the properties of vibrated concrete?

Vibrated concrete is required during the construction of structural elements such as load-bearing walls, beams, slabs or even foundations [6]. The vibrations propagated just after pouring the agglomerate make it possible to expel the air and thus obtain a better quality material [6, 7]. Concrete has pores and voids that are critical to its strength and its durability [9]. Porosity is the natural consequence of the quantity of water added to that necessary for hydration and of any voids present in the aggregates. When concrete lacks density, it suffers from the vagaries of time. It becomes porous, even friable, and disintegrates [10]. With chemical and bacteriological attacks, concrete has accelerated porosity [11]. Just as concrete that has been vibrated for a long time reduces porosity; it is in the same way that it increases the adhesion of the reinforcements to the concrete, which is the action of the strengths between the sliding of the reinforcements in the concrete.

The main aim of this work is to study the impacts of concrete vibrations on its physical and mechanical properties, and more precisely the concrete manufactured in the city of Douala Cameroon, taking into account current

recommendations on concrete vibrations. To achieve this objective, the compressive and tensile strength of the concrete of the formulations will be obtained at 7, 14 and 28 days. Then the effects of vibration on the faces of the test pieces will be analyzed. Then the adhesion strength between the concrete and steel formulations will be determined. This is followed by the determination of the density of the vibrated concrete in the wet state, as well as in the dry state.

2. Materials and Methods

2.1. Materials

2.1.1. Aggregates and Cement

The aggregates (gravel) from the Logbadjeck quarry are used, with the same the granular distribution as in [12], while sand is from the Moungo River whose technical product sheets (Granulometric curve and density parameters) are available in the Appendix I.

According to cement, that of CPJ 35 produced by CIMAF is used. This cement is made from clinker and additions such as limestone or ash.

2.1.2. Formulation of Specimens

In order to obtain the adequate consistency of the material the slump test is used here to formulate the concrete [13]. Two options for illustrating the slump of the mortar obtained are thus possible. The first one consists of increasing the fluidity of the cement matrix by increasing the Water/Cement (W/C) ratio. The second corresponds to modifying the volume of the cement paste according to that of the granular skeleton, but for the formulations the second option has been chosen, that is maintaining a constant fluidity of the cement matrix while maintaining the same W/C ratio. Only the volume variations of the cement paste (or the total volume of the granular skeleton) determine the consistency of the material. Figure 1 shows plot of the evolution of the slump of the concretes obtained during the laboratory study tests.

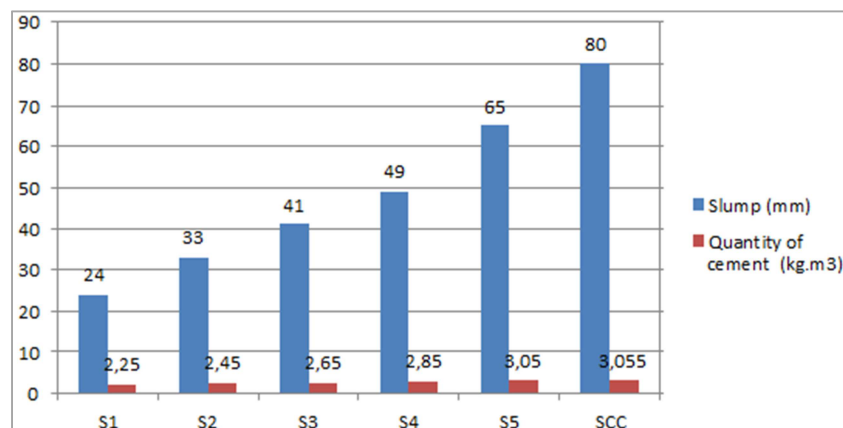


Figure 1. Slump of concrete in its fresh. The consistency classes defined by standard NF EN 206-9 are recalled [13, 14].

The formulations under consideration are thus representative of the limits imposed by the standards (NF EN

206-9, 2010). They are all representative of construction sites apart from the S1 consistency. The implementation of

concrete of this consistency remains delicate since it has very limited spreading under the sole effect of gravity. Its application is reserved for unreinforced elements such as cleaning concrete, although external help is required to spread it.

Conventionally, the pouring of concrete structural elements on construction sites is carried out from a concrete skip to which a discharge chute is attached. This has sufficient flexibility to distribute the material throughout the formwork. See Figure A2 of the appendix showing the construction site of a R+10 type building in Bonapriso town of Douala. In addition, the presence of metal reinforcements forms obstacles during the fall of the fresh concrete. They then ensure a random trajectory of the material throughout its journey.

The formulations, called S1, S2, S3, S4, S5 and self-compacting concrete (SCC) are directly linked to the consistency of the material measured from the slump test for S1 to S4 concretes or the spreading test for SCC and S5 concretes. They are similar to the formulations of deep foundations that are not vibrated. Indeed, these contain a high quantity of cement compared to the others. The manufacturing protocol for the concrete is the same for all the mixes, while the dry particles are weighed then mixed in the following order: gravel, sand then cement. The results of formulation can be found in Table 1, in which it is obvious that for constant value of W/C, the quantity of water and the slump increase with the quantity of cement.

Table 1. Concrete formulations.

Consistency class	S1	S2	S3	S4	S5	SCC
Sand0/4mm ($kg.m^{-3}$)	5.144	4.934	4.734	4.534	4.334	4.330
Gravel 6,3/20mm ($kg.m^{-3}$)	6.752	6.727	6.477	6.257	5.757	5.756
Quantity of cement ($kg.m^{-3}$)	2.250	2.450	2.650	2.850	3.050	3.055
Water efficient (L)	1.125	1.135	1.359	1.474	1.709	1.720
Total weight	15.271	15.246	15.220	15.115	14.850	14.845
Gravel/Sand	1.31	1.31	1.31	1.31	1.31	1.31
Slump (mm)	24	33	41	49	65	80
Spreading test (E) (mm)	(A)	(A)	(A)	(A)	(A)	(E)
Water/Cement	0.50	0.50	0.50	0.50	0.50	0.50

2.2. Effects of Vibration on Density

For the dry aggregates into the container, in successive layers and without compaction (use the funnel or the hands), the metal rule is used, weigh the filled container, and then calculate the apparent density:

$$\rho = M/V \quad (1)$$

Two methods of implementation are then compared: the first with the use of a vibrating needle and the second without vibration. Each of the samples is weighed fresh. Their

dimensions are assumed to be perfectly identical to those of the molds, that is its diameter equal to 16 cm and length of 32 cm. Thus, the apparent density of the 16/32 test pieces in the fresh state can be calculated. Each value corresponds to an average obtained from three samples. Then the measurements in the fresh state are compared with the theoretical value of the density provided in the Table 2, and allowing estimating the quantity of air contained in a batch of. These results are compared with that found using the test to measure the occluded air according to the standard (NF EN 12350-7, 2001) [13].

Table 2. Entrained air measurements for the concrete formulations presented in Table 1.

Consistency	S1	S2	S3	S4	S5	SCC
Air occluded (%)	1.8	1.9	1.7	1.4	0.9	1.7

The weight W_s of the dry specimen will be obtained from the formula below:

$$DS = W_s/v \quad (2)$$

where v the volume of the test piece.

2.3. Effects of Vibration on Mechanical Resistance

After 7, 14 and 28 days of storage at room temperature, the compressive strengths on 16/32 cylindrical specimens is determined in accordance with the standards (NF EN 12390-3, 2003) and (NF EN 12390-6, 2012) [16, 17]. For compression tests, each face of the cylinders undergoes surface treatment using a grinding machine to guard against

possible defects that could disrupt the results. A cyber plus evolution hydraulic press is used, having a maximum capacity of 5000 kN in simple compression, as shown in Figure A3 of the appendix. The actuator servo setting stops the compression of the sample as soon as the maximum resistance is reached. After each test, the fracture patterns of the specimens are checked according to the standard (NF EN 12390-3, 2003).

2.4. Effects of Vibration on Porosity

This will involve placing two different test tubes in two troughs, namely one vibrated and the other not vibrated, and pouring the same volume of water, finally comparing after a

given time the volume of water having been absorbed by each of the test tubes. Then a percentage estimate will be made using the following formula:

$$P = \left(\frac{V_p}{V_t} \right) \times 100, \quad (3)$$

with V_p the pore volume and V_t the total volume. In addition with the study of densities, the pronounced contrasts is observed between the aspects of the faces of the test pieces. Thus, using an image analysis tool, it is necessary to characterize the surface of these samples.

In order to have macroscopic presentation, the faces of all the 16/32 test pieces are plotted in Figure 2. Figure 2 shows a series of samples implemented without vibration. From simple visual observations, showing that the facings of the firmest concretes are more deteriorated compared to other fluidities. Indeed, for concretes of consistency S1, S2 and S3 two categories of defects can be distinguished. The first is of the order of a centimeter in size and cover almost half of the surface. The second, more classic, corresponds to air bubbles. In addition, for self-placing S4 consistency concretes, only defects of millimeter dimensions appear.

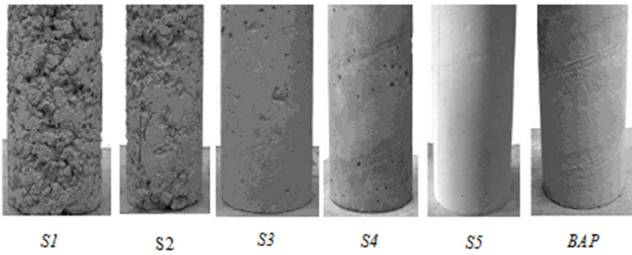


Figure 2. Examples of facings of non-vibrated 16/32 specimens.

Similarly Figure 3 shows test pieces from the same concrete formulations and manufactured with the use of pervibration. For this configuration, found that at fixed consistency, the application of vibration greatly reduces the quantity of defects in the firmest concretes (S1 to S3). Additionally the beneficial effects of the vibrating needle are less pronounced with increasing material fluidity (see Figure 3). Consequently, the evolution of the surface condition of the facings highlights the existence of the effectiveness of a vibration.

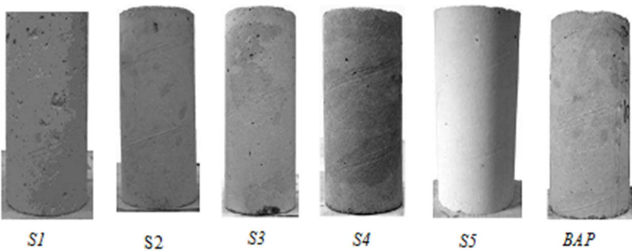


Figure 3. Examples of facings of vibrated 16/32 specimens.

The faces of concrete specimens don't naturally present as sharp a contrast as. Dips and bumps generated by defects and air bubbles form varying shades of gray on the sample surfaces. In order to study similar photos of siding, The emphasis is carried only on a central area of the image as

shown in Figure 4.

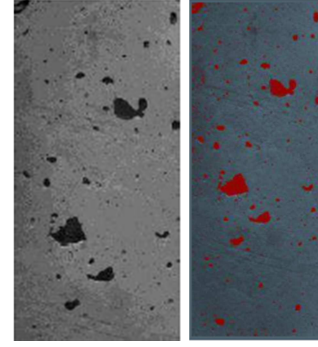


Figure 4. View of the voids on the non-vibrated 16/32 specimen.

Two study criteria are therefore chosen: the surface porosity of the sample, noted P_s , and the average diameter of the defects, noted D_M . The first corresponds to the ratio between the total surface generated by all the defects, S_V , and the surface of the image of the sample S_T , such that:

$$P_s = \frac{S_V}{S_T} \times 100 \quad (4)$$

This surface porosity term, expressed as a percentage, ranges between 0 and 100% respectively for a zero quantity of defects and a quantity of holes equal to the surface of the sample. Thus, a suitable vibration must ensure obtaining a low P_s value. Conversely, an absence of vibration should highlight surface porosity of significant value. From the surface porosity, an area free of defects is deduced such that:

$$A_{eprouv} = 1 - \frac{P_s}{100} \quad (5)$$

Thus, for very deteriorated facings, the surface porosity tends towards the value of 100% and A_{eprouv} is much less than 1. Likewise for a surface free of defects, P_s tends towards 0%, then A_{eprouv} is close to 1.

The second criterion is calculated from a weighting of the diameters of each defect in relation to the total surface area of the defects such that:

$$D_M = \frac{\sum_i^{nd} (D_i - A_i)}{\sum_i^{nd} A_i} \quad (6)$$

With D_i (cm) the diameter of the defect encountered, and A_i area of the defect, n_d : the total number of defects which varies depending on the image. In addition, the probability of the presence of defects on the surface of the samples is identical regardless of the area considered. In addition, the effect of gravity is studied from the following relationship:

$$E_{fg} = \frac{T_o}{p.g.L} \quad (7)$$

To choose a characteristic length (L), the average diameter of the defects, D_M without vibration is calculated. So, from the previous results D_M is equal to 4 cm. The following ratio is found:

$$R = \frac{T_o}{p.g.D_M} \quad (8)$$

2.5. Effects of Vibration on Steel/Concrete Adhesion: Experimental Protocol

For this study, the same concrete formulations are used, as those above, except for consistency class S4. The sample preparation device allows the preparation of concrete cubes of 15 cm side with the insertion, at halfway up, with a steel bar. This corresponds to a high-adhesion steel frame with a diameter of 14 mm (HA14). A coating system (PVC tube, see Figure 5) placed against the internal formwork faces, ensures a steel/concrete contact length equal to 80mm. Finally, solely for the purpose of ensuring easy handling of concrete samples in the hardened state, the reinforcement of length equal to 50cm is used.

The recommendations issued by RILEM (international meeting of laboratories) May 1970. Stipulate that the concrete cube measures ten times the diameter of the reinforcement. Likewise, the grip length of the bar corresponds to five times its diameter. Thus, with a sample of 15 cm side, the maximum diameter of the metal bar cannot exceed 15 mm with an adhesion length equal to 75 mm. Although the dimensions of the samples respect the RILEM recommendations, the adhesion zone does not agree. In fact, it should be located in the heart of the concrete block and not near a wall. Therefore, the results found will allow a qualitative comparison between the multiple trials. On the other hand, establishing a precise quantitative comparison with the literature will be more delicate.

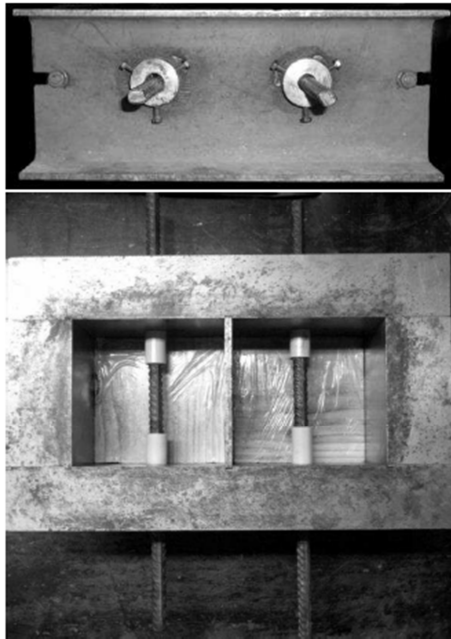


Figure 5. Molds for casting steel/concrete adhesion samples Front view (top) Top view made at the host site.

Measure of the Steel/Concrete Adhesion

In order to measure the steel/concrete adhesion, a metal bar tearing device is used. This consists of a high-adhesion steel bar cast in concrete. The sample making device allows the preparation of concrete cubes measuring 15 cm on each side with the insertion, halfway up, of a steel bar, as shown in

Figure 6. This corresponds to a high-adhesion steel frame with a diameter of 14 mm (HA14). A coating system placed against the internal formwork faces ensures a steel/concrete contact length equal to 80mm.

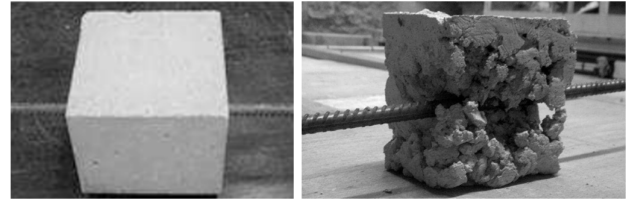


Figure 6. (left) Preparation of the specimen before carrying out a test; (right) Configuration sample with concrete of consistency S1 and implemented without vibration.

Note that, in the case of consistency class S1 concrete without vibration with a sail type, the fluidity of the material was not sufficient to coat the reinforcement and maintain it upon demolding. For these samples, regardless of the maintenance of the steel bar, the facing appearance is very degraded. (See Figure 6 (right)). The establishment of friction between the concrete and the crenellations of the reinforcement produces mechanical adhesion and allows an increase in resistance to tearing. As soon as this is exceeded, the relative displacement between the metal bar and the concrete increases sharply with a sudden drop in resistance.

2.6. Mechanical Behavior of a Needle

From manufacturers' data, the amplitude of the vibrating needles varies as a function of their diameter for electric vibrators. It is found that the amplitude of the vibrators increases proportionally with their diameter, as shown in Tables of appendix 4. However, this coefficient proportionality varying from one manufacturer to another, the relationship between the diameter and the amplitude must be modulated depending on the material supplier.

Furthermore, suppliers of vibrating needles stipulate that the density of the material used for the design of the unbalance remains constant with the increase in diameters.

Likewise, by assuming that the variations in the total mass of the vibrating body are negligible compared to those of the unbalance, thus the increase in amplitude is induced, to first order, by an unbalance of increasing dimensions generating a mass gain, such as.

$$a = km_b \quad (9)$$

where m_b is the mass of the unbalance. It has been proved that (Geoffray, 2008) the centrifugal Strength of a needle is proportional to the mass of the vibrated concrete such that:

$$F_c = a \cdot (2\pi f)^2 m_v \quad (10)$$

m_v being the mass of the vibrating needle (m). The mass of vibrated concrete can be expressed from the product of its volume and its density, such that $m_v = \rho_b \cdot V_v$. In addition, from a dimensional point of view, the vibrated volume is proportional to the product of the diameter D of the vibrator

and its height, such that $Vv = \frac{\pi}{4} D^2 \cdot H_V$. Therefore, the previous equation becomes:

$$F_C = a \cdot \rho_b \cdot \pi^3 D^2 f^2 H_V \quad (11)$$

It is obvious that an electric vibrating needle measuring 25 mm in diameter and with a frequency of 200 Hz according to the technical sheet is also used here (See Figure 7).



Figure 7. IREN 57 vibrator.

2.7. Measure of the Diameter of Action of the Vibrators

The diameter of action of the vibrators is measured, from the penetration of markers placed on the surface of the cementitious materials. The cement pastes are all prepared following the same protocol as described above. The test protocol for measuring the action radius of the vibrator is identical regardless of the cementitious material studied. The test is only performed once. Firstly, the material after mixing is then poured into the container. The vibration is applied for a sufficiently long time so that it reaches its maximum speed and no temporal evolution of the increase in the action diameter is observed. Then the vibrating needle is extracted from the working material. Finally, the action diameter is measured. The figure 8 shows the measurement of the action radius of IREN 57 immersed in a cement paste with a ratio $E/C=0.5$.

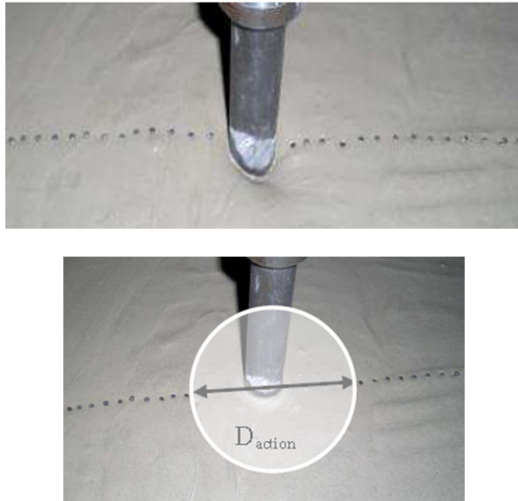


Figure 8. Cement paste. (left): State before vibration. (right): State after vibration, with at $W/C=0.5$ and with a frequency equal to 100 Hz.

2.8. In Situ Study of Beams at Scale: Presentation of the Experiment

This test is carried out within the host site: construction

project of a R+10 type building in Bonapriso. The formulations of the concretes have a consistency S3 and S4. For the study of horizontal elements of constant dimensions with concretes of varied consistencies, from the postulated of the factor 10 between the action diameter and the diameter of the vibrator, a beam whose length is significantly greater than this coefficient is chosen. In addition, the pouring capacity of this test is limited to 150 liters, the maximum volume of a batch manufactured at one time. In order to respect these two criteria, the studied beam has the following dimensions: $1.50m \times 0.40m \times 0.20m$ (length/height/width).

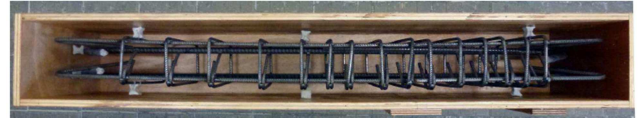


Figure 9. Reinforcement cage placed inside a wooden formwork with covering blocks.

Similarly, these tests aim to study the influence of reinforcement on the transmission of vibration. In fact, the reinforcing cage (see Figure 9) tested is composed of a so-called loose density with 2HA20 at the level of the lower layer and a so-called dense density with, in addition to the previous steels, a second layer with 2HA14. In addition, the transverse steels correspond to frames formed by HA8 steels spaced every 12 cm. The vibrators available on this site have a diameter from 50 mm to 60 mm respectively for the construction of the said building. In addition, the vibrating needle is immersed only in the center of the samples for a period of 30 s. At the same time, within the same reception site, the pouring is witnessed of a large lintel: $3.70m \times 1.00m \times 0.45m$ (Length/Height/Width). Unlike other samples, the implementation of these elements is carried out according to traditional implementation rules.

From simple visual observations, the diameter of action of the vibrator is estimated. To vibrate concrete correctly, two components are essential. The first corresponds to the spacing between the action zones of the vibrator while the second constitutes the duration of depression between the application points.

2.9. Influence of Vibration Duration

Recent work has highlighted the digital prediction capabilities of formwork filling for concrete through reinforcing cages of various dimensions [14]. However, they only consider the flow of material under the effect of gravity [15]. Consequently, the duration necessary for concrete to compact when subjected to pervibration is first studied.

The compression characteristic time T , of a formwork as a function of the rheological properties of a concrete such as a viscosity/stress ratio:

$$T \approx \frac{\mu_p}{\tau} \quad (12)$$

From a dimensional point of view, the stress in concrete is equivalent to the product of its density, the earth's gravitational acceleration and a characteristic length of the flow. In order to take into account the cavities present at the

level of the facing of the material before the application of a vibration, as characteristic distance the average diameter of these defects, noted D_M is chosen. Finally, this compression time is modeled by TC1, leading the Ratio (12) to:

$$T_{C1} \approx \frac{\mu_P}{P_{g.DM}}. \quad (13)$$

In addition, for traditional concrete, the orders of magnitude of the parameters of this equation are known. Indeed, its viscosity is of the order of 102 Pa. Its density is of the order of 103 kg.m^{-3} . Thus, the time required for concrete to compact under the effect of pervibration would be of the order of 1 s to 10 s. However, this duration doesn't allow to obtain quality facings. In fact, millimeter-sized air bubbles always remain on the surface and at the heart of the material. Therefore, a second characteristic time is defined to describe the duration necessary to allow the entrained air to rise.

2.10. Bubble Rise Time

The same dimensional approach is kept, except for the distance term characteristic of the flow. The average diameter of the defects before vibration D_M is replaced by the diameter of the air bubbles obtained D_A in Eq. (13).

For this study, formwork of the same dimensions is chosen as the one above in order to ensure that the volume of the material is completely subjected to the applied vibration. All formwork faces are made of wood (Cf. Figure 9).

For these tests, a traditional laboratory vibrating needle is used whose mechanical characteristics in air correspond to a fixed frequency of 200 Hz. Ordinary self-compacting consistency class S2 concretes are tested. First, the mold is filled in its entirety. Then the operating vibrating needle is plunged into the center of the element. Varying vibration durations between five seconds and sixty seconds are applied. These vibration times correspond to the duration for which the vibrator is located within the material, including descent and rise of the material.

Then, from a viewing, the time necessary for the concrete to fill the surface cavities (that is compact) as well as the time for the air bubbles to rise is identified. As hypothesis, the duration of the bubbles rising against the facing is equal to that at the core while the effects of surface tension probably slow down the bubbles.

3. Results and Discussion

In this section the results obtained from the methodology presented in the previous section are presented, then interpreted, thus allowing bringing answer to research questions.

3.1. Effects of Vibration on Mechanical Resistance

3.1.1. Supplement to the Experimental Protocol

After 28 days of storage at room temperature, the simple compressive strengths is determined on 16/32 cylindrical specimens [18]. For simple compression tests, each side

cylinders undergo surface treatment using a grinding machine to guard against possible defects that could disrupt the results found. A hydraulic press with a maximum capacity of 500kN in simple compression is used. The actuator servo setting stops the compression of the sample as soon as the maximum resistance is reached. After each test, the fracture patterns of the specimens are checked.

3.1.2. Simple Compressive Strength

In Figure 10 the mechanical resistance in simple compression of the 16/32 specimens is plotted as a function of the consistency class of the concrete at 7, 14 and 28 days according to Table A3 in the appendix. Then the two implementation modes are compared, with the aim of minimizing errors. The mechanical resistance values thus correspond to the average of three tests.

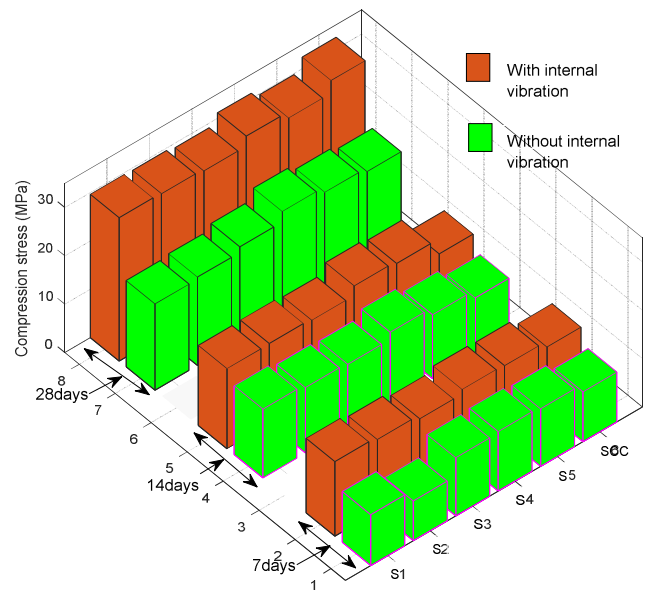


Figure 10. Compression stress on cylindrical specimens 16/32 at 7, 14 and 28 days depending on the consistency class of the material and the application of vibration in the fresh state.

The results found show that the mechanical stress in compression decreases considerably for concrete of consistency S1 in a non-vibrated configuration. It is obvious that the application of vibration allows for the majority of the measurements to reduce the dispersion of the results. The results found also show that the mechanical resistance in compression decreases considerably only for concrete of consistency S1 in non-vibrated configuration. On the other hand, for all the other formulations tested, none presents the expected reduction in resistance despite an absence of vibration in the fresh state.

3.2. Simple Tensile Strength

Figure 11 shows the mechanical strength in simple traction of the 16/32 specimens as a function of the consistency classes of the concrete formulations, referring to Table A4 in the appendix.

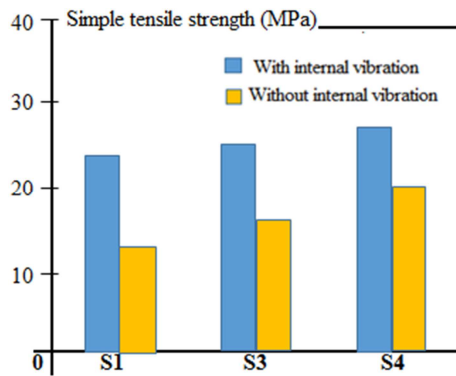


Figure 11. Tensile stress on cylindrical specimens 16/32 at 28 days depending on the consistency class of the material and the application of vibration in the fresh state.

These results show the same trends as those highlighted with the simple compressive strength tests. In fact, only consistency class S1 in non-vibrated configuration presents a reduction in mechanical resistance in simple traction. It is

obvious that the traction tests aren't carried out for the S2, S5 and SCC formulations, since it is assumed that these concretes have the same tendencies in simple tension as in simple compression.

3.3. Effects of Vibration on the Appearance of the Facing

Figure 12 shows the evolution of the surface porosity of the facings as a function of the consistency class using Table A4 in the appendix.

These results highlight two main findings. First of all, in the absence of vibration, the surface porosity decreases sharply with the increase in the fluidity of the concrete in the fresh state. In fact, two orders of magnitude separate the surface porosity of concrete of consistency S1 and that of consistency S4, respectively equal to 64% and 0.1%.

At the same time, this reduction is more pronounced for sufficiently fluid materials, i.e. from consistency class S4. Thus, the results found show a significant evolution depending on the mode of implementation.

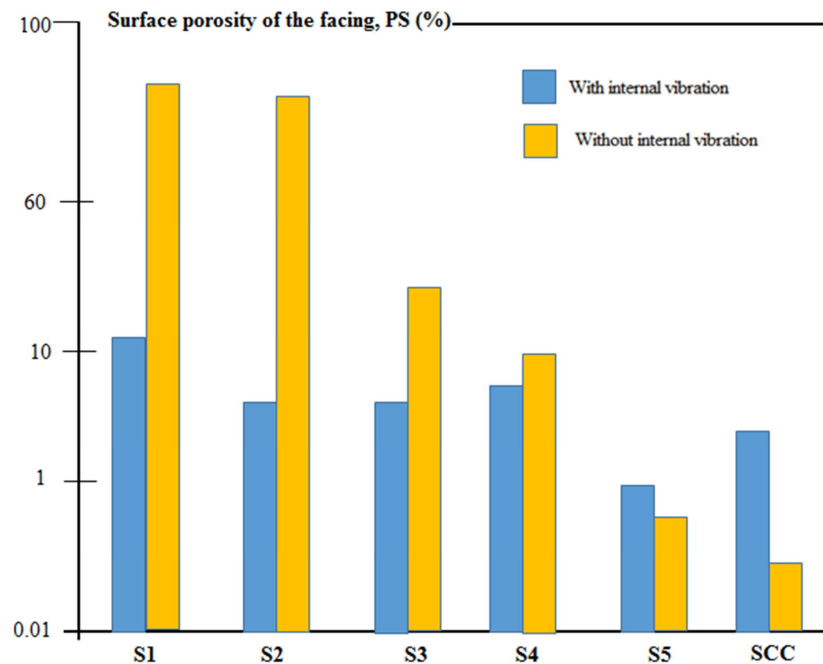


Figure 12. Surface porosity measured by image analysis on concrete samples at 28 days.

Secondly, whatever the consistency of the material, vibration ensures a facing with a limited amount of defects. Indeed, the surface porosity is always approximately equal to 1%. Alongside these beneficial effects, the same Figure 12 shows that for SCC, the use of vibration tends to increase the surface porosity. Finally, for a very fluid consistency from type S4, vibration does not seem to affect this type of material.

Figure 13 shows the second image analysis criterion, namely the evolution of the average diameter of the defects as a function of consistency, using Table A6 in the appendix. the same trends are found as those presented previously. Indeed, in the absence of vibration, the average diameter of the defects decreases sharply with the increase in fluidity up

to a minimum value approximately equal to 1mm. In addition, at fixed consistency, the use of vibration ensures an average diameter of defects smaller than that of non-vibrated samples. However, unlike surface porosity, the average diameter of defects in vibrated samples isn't constant. Despite an identical protocol depending on consistency, DM after vibration also decreases with increasing fluidity. Finally, this study criterion also shows that concretes with very fluid consistency (S4) do not seem to be affected by an absence of vibration. Indeed, whatever the implementation mode, a similar value is obtained for their average diameter of defects.

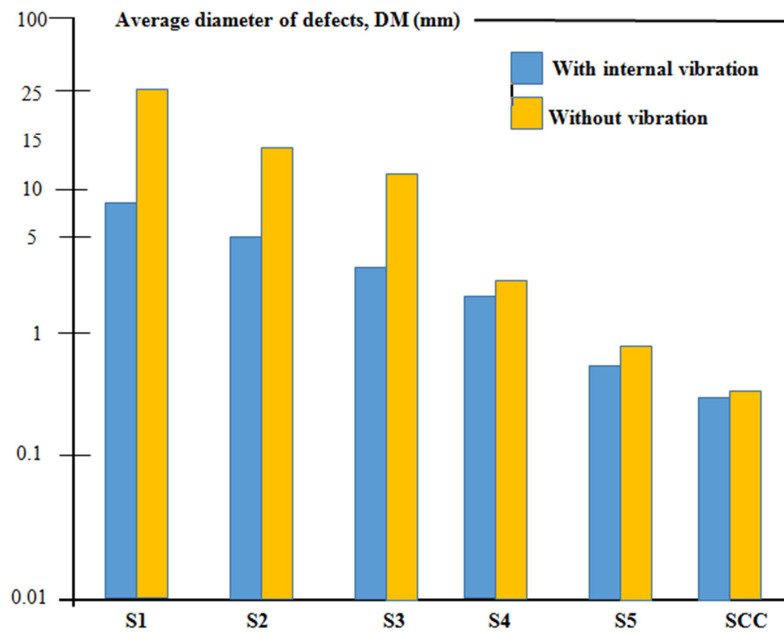


Figure 13. Average diameters of surface defects measured by image analysis on hardened concrete samples.

It is obvious that the surface porosity or the average diameter allows to highlight the influence of vibration in the fresh state.

3.4. Effects of Vibration on the Porosity of Concrete in the Formulations

The porous nature at the core of the specimens is used for

characterizations, using the protocol stated above consisting of immersing the test tubes in troughs containing measured and weighed water. The analyzes carried out after 24 hours allow the plotting in Figure 14 the core porosity, according to the method of implementation, referring to Table A5 in the appendix.

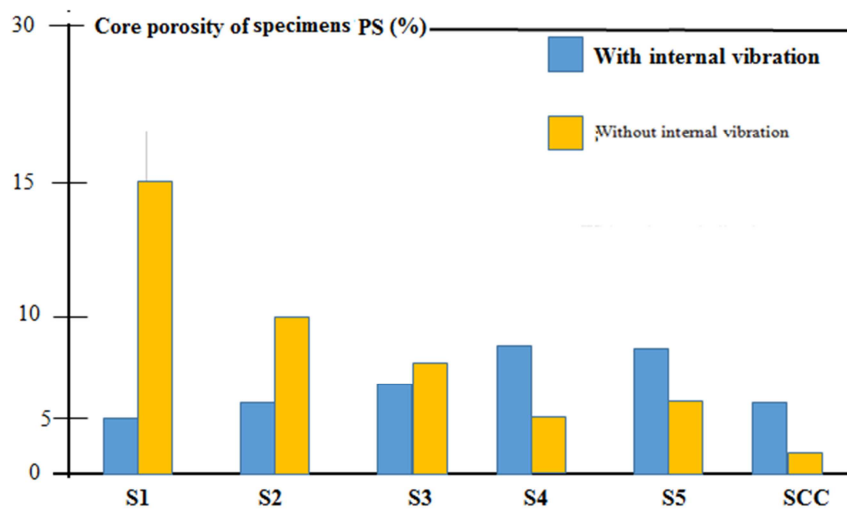


Figure 14. Core porosity of the test pieces at 28 days.

These results show that concretes of consistency S1 and S2 in the non-vibration state absorb more water unlike other types of consistency. The same results also show that according to the formulations used, the highest absorption percentage is 15% and is linked to concretes of formulation S1 in non-vibrated configuration.

3.5. Effects of Vibration on Density

In Figure 15 the evolution of the apparent density of the

16/32 specimen is plotted as a function of the consistency class of the concrete using Table A7 in the appendix. Two methods of implementation are compared: the first with the use of a vibrating needle and the second without vibration.

As one can see, the vibrations have little effect on the apparent density of concrete, contrary to what was possible to anticipate. Indeed, for 16/32 specimens manufactured with concretes of consistency class S1 to S3, the results found show a reduction in density ranging between 12% to 5% when they are not vibrated following traditional

recommendations.. However, for the most fluid concretes, the density of the samples is similar regardless of the implementation method. Indeed, the absence of pervibration does not seem to reduce the density of these concretes.

Furthermore, for SCC with a traditional implementation,

i.e. without vibration, the apparent density corresponds to that predicted theoretically. On the other hand, the use of pervibration does not seem to affect the samples since their density is similar to that of non-vibrated specimens.

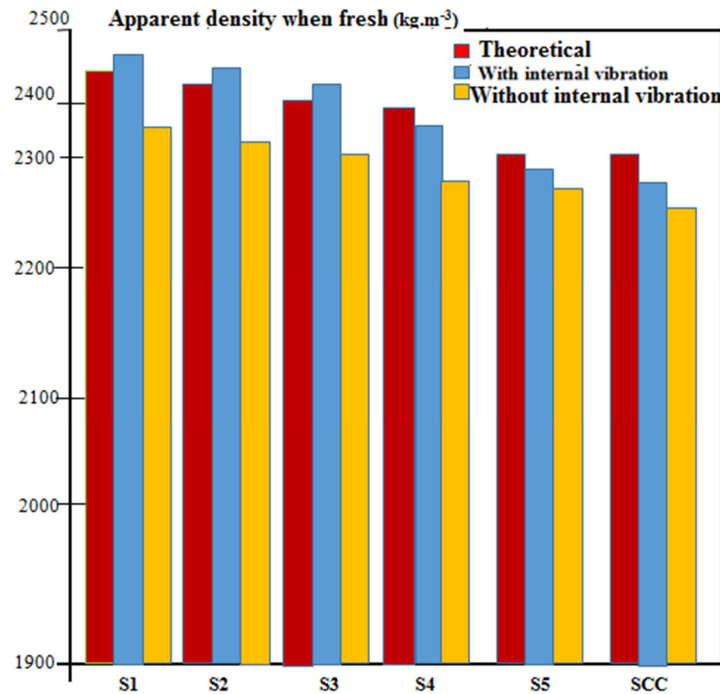


Figure 15. Apparent densities of the 16/32 specimens depending on the implementation in the fresh state.

3.6. Effects of Vibration on Steel/Concrete Adhesion

Figure 16 shows the total steel/concrete bond Strength for a beam-type configuration as a function of consistency using Table A9 in the appendix.

In the absence of vibration, the resistance to tearing is almost zero for concrete of consistency S1. Steel/concrete adhesion increases with the fluidity of the formulations tested. Furthermore, for consistencies S1 to S3 implemented with the use of pervibration, an average value close to 40kN is obtained. However, for vibrated concrete, the adhesion of materials with high fluidity (S4 to AP) is lower than that of other consistencies.

In fact, the SCC formulations limit the rise of water in the material in its fresh state. Thus, a layer of water forms under the reinforcements and reduces the contact surface between the steel and the concrete. However, this phenomenon is especially pronounced for steels located in the upper part within high vertical elements.

Figure 17 shows the total steel/concrete adhesion Strength for a sail type configuration as a function of consistency with reference to Table A10 in the appendix. As for the beam type configuration, in the absence of vibration, the resistance to tearing is almost zero for the firmest concretes. On the other hand, it increases with the fluidity of the formulations tested. In addition, for consistencies S1 to S4 implemented with the use of pervibration, an average resistance lower than for the previous

configuration is obtained, with a drop of around 10kN.

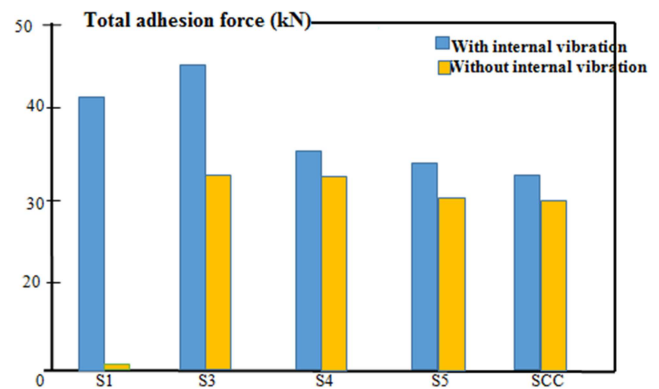


Figure 16. Adhesion resistance depending on the consistency of the concrete in the case of a beam type configuration.

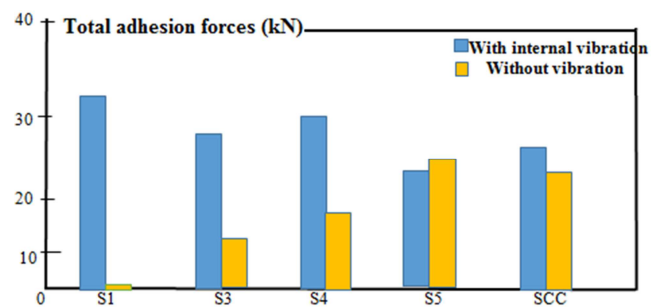


Figure 17. Adhesion resistance depending on the consistency of the concrete in the case of a sail type configuration.

It should be noted that, in the case of consistency class S1 concrete without vibration with a sail type, the fluidity of the material was not sufficient to coat the reinforcement and maintain it upon demolding. For these samples, regardless of the maintenance of the steel bar, the facing appearance is very degraded.

In Figure 18, shows the dimensionless ratio of the maximum resistance Strength to the tearing of the reinforcements in the concrete between a vibrated concrete and a non-vibrated concrete as a function of the consistency with reference to Table A7 in the appendix. The value 100% is reached when the pull-out Strength of the non-vibrated samples is identical to that of the vibrated samples. These results show the need to apply pervibration to obtain quality adhesion for all classes of consistencies tested, except for the two most fluid (S5 and SCC). This pull-out test highlights the quality of the steel/concrete interface. Indeed, when the concrete does not perfectly coat the steel, the contact surface between these two materials decreases (see Figure 18).

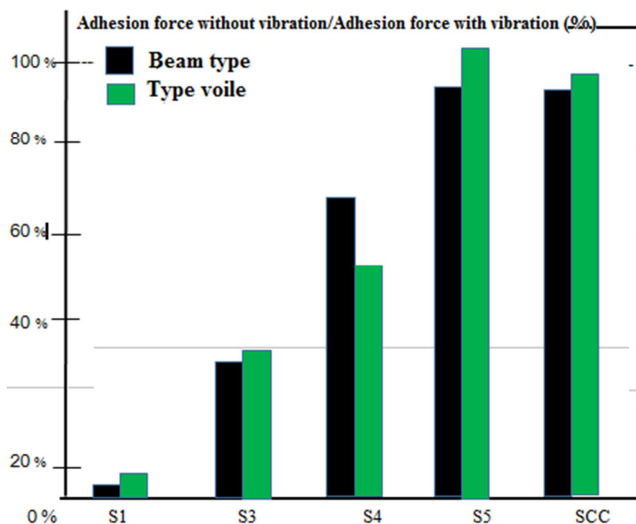


Figure 18. Dimensionless ratio of the adhesion force of the reinforcement in the concrete between non-vibrated concrete and vibrated concrete depending on its consistency.

Finally, from a practical point of view, the following conclusions are proposed:

1. Class S1 to S3 concrete must be vibrated otherwise the properties will decrease significantly. In addition, the steel/concrete adhesion is close to zero for non-vibrated S1 consistency concrete.
2. For S4 consistency concrete, if the material is not exposed to an aggressive environment, it would be possible not to apply vibration because its resistance would not be reduced. However, it would be necessary to take into account a notable reduction in the adhesion of the reinforcements when designing the structures. Be careful, the quality of the facings in the absence of vibration would be poor, thus favoring the penetration of chlorides or carbonation. Therefore, it seems reasonable to maintain vibration during the pouring of concrete with class S4 consistency.
3. Vibration does not seem necessary for concrete of S4

consistency and it does not improve the properties of SCC (already known point). In addition, it would be detrimental to vibrate SCC because there is a strong risk of segregation even if this was not highlighted in the formulation of the SCCs tested during the tests. It is important to note that the study of facings constitutes a non-destructive and inexpensive test unlike the verification of steel/concrete adhesion.

3.7. Formwork Filling Time

In Figure 19 the formwork filling time is plotted as a function of the consistency of the concrete. According to experimental findings, this time decreases with the increase in the fluidity of the material. It is maximum for S1 consistency class concretes with a duration of around 15s and tends towards a value close to 5s for the S4 consistency formulation.

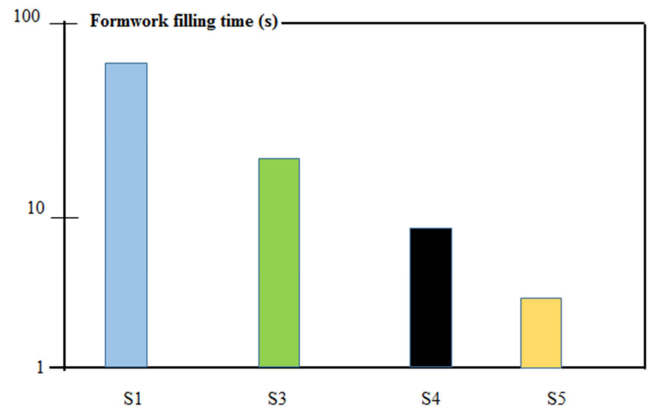


Figure 19. Duration of filling of LBR construction site experimental formwork.

3.8. Bubble Rise Time

Figure 20 shows the measurement of the air bubble rise time as a function of the consistency of the concrete. The time required for the air bubbles to rise to the surface is maximum for the firmest concretes, with a time of around a hundred seconds and decreases with the increase in their fluidity until reaching a few dozen of seconds.

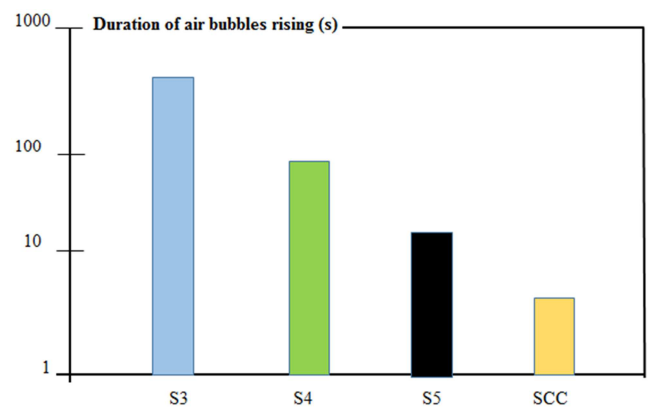


Figure 20. Duration of air bubbles rising. LBR construction site experimentation.

The experimental results found of filling cavities and raising air bubbles seem to be in agreement with the approach used. Thus, the ratios of times TC1 and TC2 (see Eqs. 10. and 11) can describe to first order, the two characteristic times. The times for air bubbles to rise to the surface can reach several tens of seconds. These vibration times seem relatively long compared to practice. This may be due to the presence of the walls of the mold.

From a dimensional analysis and the application of orders of magnitude, two characteristic times can be distinguished for implementing concrete.

The first, TC1, has a duration of between 1 and 10 s and corresponds to the time necessary for compacting the material to ensure, in the hardened state, quality mechanical properties. The second, TC2, identifies a time for air bubbles to rise to the surface of between 10 and 100s. It allows obtaining a good quality of facing.

4. Conclusion

In this work, the effect of vibration on the physical and mechanical properties of concrete in the city of Douala Cameroon is studied, through several axes of study. Firstly the macroscopic properties in the hardened state of concretes of varied rheologies (i.e. from a slump of 4 cm to the fluidity of self-compacting concrete) are studied, in two configurations: vibrated and non-vibrated. All of the tests were carried out on samples whose reduced size combined with a suitable choice of pervibrator allowed to ensure that all of the material tested was affected by vibration. The vibrations applied were in accordance with existing international recommendations. The compressive strength on these samples are then measured from 7 to 28 days, and the simple tensile strength. The results found confirmed that all properties were improved by vibration in the case of the firmest concretes while vibration was not necessary or even harmful in the case of self-compacting concretes. The faces of the test pieces (surface porosity) are then analyzed. It was therefore a question, after drying the specimen, of making an observation on the defects of the different specimens according to the two configurations (vibrated and non-vibrated). it was noted that the firmest concretes present more defects compared to those tending towards SCC (S4.....).

Appendix

Appendix I. Characteristics of the Sand from Mounjo River

Table A1. Extract of the granulometric composition of Mounjo sands.

Materials	Passing particles the sieve of 5mm (%)	Passing particles the sieve of 1.25mm (%)	Passing particles the sieve of 315 μ m (%)	Passing particles the sieve of 80 μ m (%)
Sand of Mounjo	98,95	62,43	5,72	0,29

Table A2. Density parameters of the sand of Mounjo.

Dry density, (g/cm ³)	Void index, e	Porosity, n (%)	Absolute density, (g/cm ³)
1.51	0.74	42	2.64

However, unlike the surface porosity, the average diameter DM of defects in vibrated samples is not constant at the same value. However, depending on the consistency, DM after vibration also decreases with increasing fluidity. So whatever the consistency of the material, vibration ensures a smooth facing, with a limited quantity of defects. Alongside these beneficial effects, the results show that for SCC, the use of vibration tends to increase surface porosity. Finally, for a very fluid consistency of type S4, vibration does not seem to affect this type of material.

It is obvious that in the absence of vibration, the resistance to tearing is almost zero for concretes of consistency S1. Steel/concrete adhesion increases with the fluidity of the formulations tested. In addition, for consistencies S1 to S3 implemented with the use of pervibration, an average value close to 40kN is obtained. However, for vibrated concrete, the adhesion of high fluidity materials (S4 to SCC) is lower than that of other consistencies. In fact, SCC formulations limit the rise of water in the material in its fresh state. Thus, a layer of water forms under the reinforcements and reduces the contact surface between the steel and the concrete. However, this phenomenon is especially pronounced for steels located in the upper part within high vertical elements.

The experimental results found allowed to identify two characteristic times associated with the vibration of the material by a pervibrator. The first, of the order of a few seconds for the concrete tested, corresponds to the time necessary to compact the material in order to remove major centimeter defects. The second is associated with a rise time of millimetric air bubbles to the surface of the order of several tens of seconds. This allows obtaining a good quality of facing.

ORCID

<https://orcid.org/0000-0001-6440-3579> (Fabien Kenmogne)

Conflicts of Interest

The authors declare no conflicts of interest.

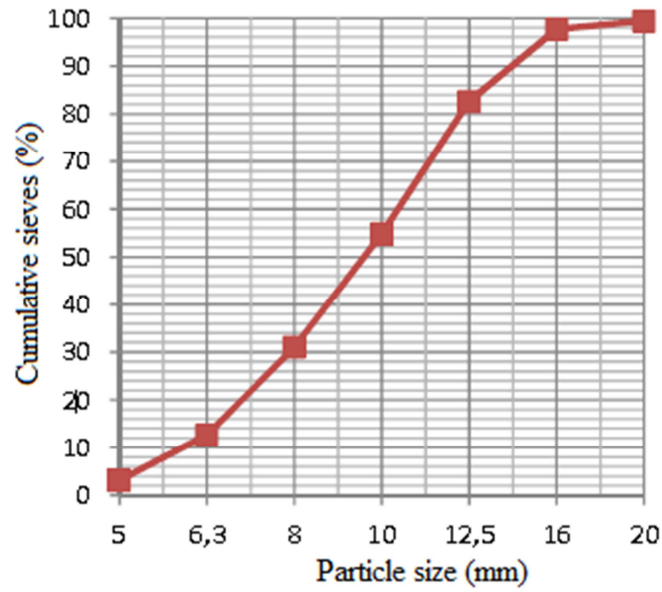


Figure A1. Granulometric curve of Moungo sands.

Appendix II. Concreting at the Construction Site in Bonapriso Town in the City of Douala

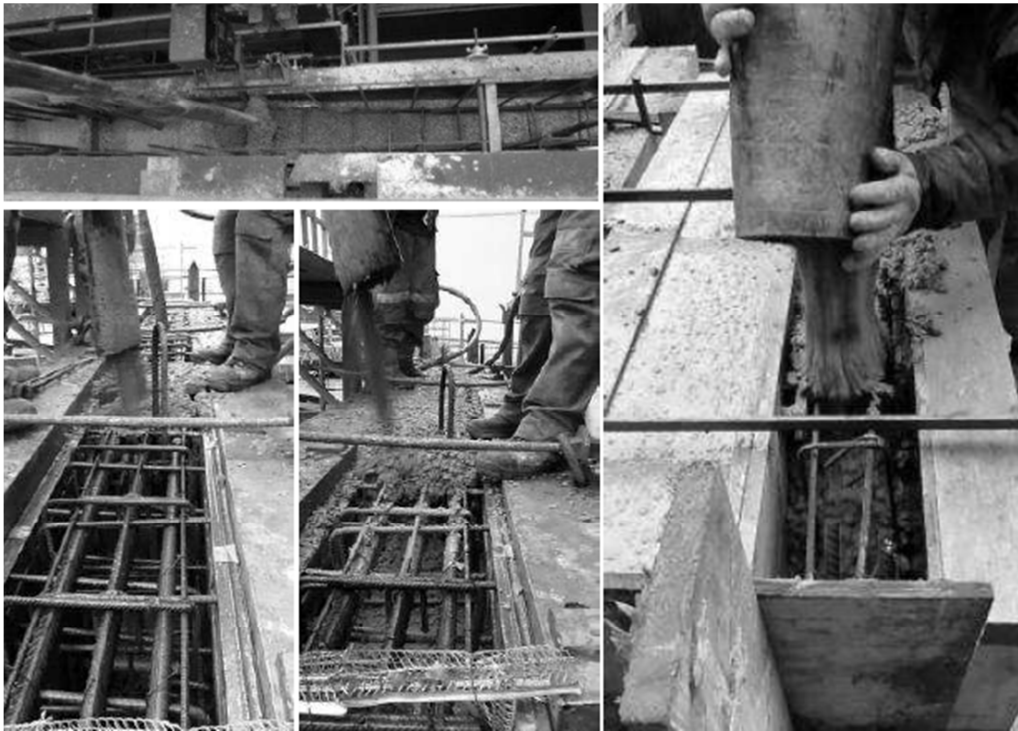


Figure A2. Concreting at the construction site of a R+10 type building in (Bonapriso).

Appendix III. Mechanical Properties

Table A3. Constraints obtained from the tests and formulations.

Days	Sample	Not vibrated		Vibrated	
		Strength (kN)	Stress (Mpa)	Strength (kN)	Stress (Mpa)
	S1.1	35.354	11.342	49.452	15.865
	S1.2	33.258	10.669	49.854	12.786
	S1.3	29.357	9.418	49.258	11.632
	Average	32.656	10.476	49.254	15.427
	S2.1	30.365	9.741	45.954	14.743
	S2.2	26.324	8.445	40.254	12.272

Days	Sample	Not vibrated		Vibrated	
		Strength (kN)	Stress (Mpa)	Strength (kN)	Stress (Mpa)
7 days	S2.3	20.245	6.495	36.254	11.631
	Average	25.644	8.227	40.154	14.882
	S3.1	38.954	12.497	46.125	14.797
	S3.2	36.324	11.653	44.258	14.198
	S3.3	37.321	11.973	41.025	13.161
	Average	37.533	12.041	43.802	14.052
	S4.1	38.996	12.510	51.125	16.401
	S4.2	37.898	12.158	49.123	15.759
	S4.3	38.458	12.338	47.125	15.118
	Average	38.450	12.335	49.124	15.009
	S5.1	37.698	12.094	49.254	15.801
	S5.2	35.324	11.332	44.025	14.124
	S5.3	38.321	12.294	45.021	14.443
	Average	37.144	11.906	46.100	14.789
	S6.1	33.247	10.666	45.354	14.550
	S6.2	32.148	10.313	39.985	12.820
14 days	S6.3	30.954	9.930	41.321	13.256
	Average	32.149	10.303	42.220	13.542
	S1.1	33.248	10.666	57.654	18.496
	S1.2	35.364	11.345	54.215	17.393
	S1.3	36.369	11.667	55.125	17.685
	Average	34.993	14.226	55.660	17.856
	S2.1	44.654	14.325	61.236	19.645
	S2.2	40.364	12.949	56.547	18.141
	S2.3	41.687	13.374	53.214	17.072
	Average	42.235	13.549	56.999	18.286
	S3.1	45.352	14.549	60.654	19.459
	S3.2	39.547	12.687	59.547	19.103
	S3.3	39.024	12.519	61.541	19.743
	Average	41.307	13.251	60.580	19.435
	S4.1	48.245	15.478	68.154	21.865
	S4.2	45.214		67.698	
28 days	S4.3	44.210		66.325	
	Average	45.889	14.722	67.392	21.620
	S5.1	41.025		65.323	
	S5.2	42.125		62.147	
	S5.3	40.896		63.987	
	Average	41.348	13.265	63.752	20.452
	S6.1	39.987		63.123	
	S6.2	35.236		60.357	
	S6.3	33.268		59.965	
	Average	36.163	11.601	61.148	19.617
	S1.1	45.362		93.657	
	S1.2	41.369		89.368	
	S1.3	49.354		94.012	
	Average	45.361	16.552	92.345	29.626
	S2.1	46.315		92.254	
	S2.2	44.258		92.365	
	S2.3	46.458		91.025	
	Average	45.677	16.654	91.881	29.477
	S3.1	40.147		90.547	
	S3.2	43.687		89.369	
	S3.3	49.965		91.875	
	Average	44.599	16.308	90.597	29.065
	S4.1	56.248		99.354	
	S4.2	57.965		96.357	
	S4.3	56.951		95.345	
	Average	57.054	18.304	97.018	31.125
	S5.1	48.965		95.364	
	S5.2	49.987		93.140	
	S5.3	48.985		89.969	
	Average	49.312	17.820	92.824	29.779
	S6.1	41.965		85.670	
	S6.2	42.129		87.358	
	S6.3	43.954		83.254	
	Average	42.682	14.693	85.427	32.406

Table A4. Simple tensile stresses at 28 days.

Days	Samples	Not vibrated			Vibrated	
		Area (mm ²)	(Strengths kN)	Stress (Mpa)	Strengths (kN)	Stress (Mpa)
28 Days	S1	3119.665	35.362	11.335	83.657	26.816
	S3	3119.665	40.147	12.869	89.547	28.704
	S4	3119.665	56.248	18.035	90.354	28.962

*Figure A3. Hydraulic presses used.**Figure A4. Preparation of the Test Specimens.*

Appendix IV. Physical Properties

Table A5. Percentage Table of Porosity of the Test Pieces.

Specimens	Total porosity (%)		Core porosity (%)	
	Not vibrated	Vibrated	Not vibrated	Vibrated
S1	89	8	15	5
S2	60	5	10	6
S3	10	4	8	7
S4	3	3	5	8
S5	1	2	3.5	8
SCC	0	2	3	6

Table A6. Average diameter of defects.

Specimens	Diameter (mm)	
	Not vibrated	Vibrated
S1	25	8
S2	15	5
S3	10	4
S4	1	3
S5	0.1	1
SCC	0.01	0.01

Table A7. Density values.

Formulations	Densities		
	Theoretical	Apparentes Not vibrated	Apparentes vibrées
S1	2422	2375	2460
S2	2418	2370	2450
S3	2414	2367	2430
S4	2410	2350	2400
S5	2356	2309	2350
SCC	2355	2308	2310

Table A8. Steel/Concrete adhesion table.

Formulations	Strength adhesion (kN)	
	Not vibrated	Vibrated
S1	0.09	40
S3	33	45
S4	34	36
S5	30	35
SCC	33	34

Table A9. Steel/Concrete adhesion table, beam type.

Formulations	Strength adhesion (kN)	
	Not vibrated	Vibrated
S1	0.01	33
S3	10	29
S4	18	30
S5	28	27
SCC	26	29

Table A10. Steel/Concrete adhesion table, sail type.

Formulations	Strength adhesion (%)	
	Not vibrated	Vibrated
S1	5	5
S3	38	35
S4	47	65
S5	110	98
SCC	99	98

Appendix V. Characteristics of Commercially Available Vibrating Needles Electric Vibrators Available in Douala Cameroon and Used in These Studies

Table A11. Electrical vibrators.

Denomination	Diameter (mm)	Frequency (Hz)	Amplitude (mm)	Centrifugal strength (N)
AX36	36	200	2.10	1350
AX40	40	200	2.50	1400
AX48	48	200	2.70	3400
AX56	56	200	3.10	4300
AX65	65	200	3.40	6700
AX90	90	100	5.00	NC
SMART Ee28	28	200	0.9	1000
SMART E40	40	205	2.8	1600
SMART E48	48	205	3.2	2700
SMART E56	56	205	3.5	4600
SMART 40	40	200	2.6	1600
SMART48	48	200	2.8	2700
SMART 56	56	200	3.2	4600
SMART 65	65	200	3.5	6000
Vibrator 40	40	200	0.84	1000
Vibrator 50	50	200	0.86	2000
Vibrator 60	60	200	0.78	3000

Table A12. Mechanical Vibrators.

Denomination	Diameter (mm)	Frequency (Hz)	Amplitude (mm)	Centrifugal strength (N)
AA27	25	200	0.30	570
AA37	39	200	0.55	2000
AA47	50	187	0.69	3800
AA67	63	175	0.84	4300
AA77	75	153	1.20	4700
AT29	29	200	0.80	950
AT39	39	200	1.00	1750
AT49	49	200	1.20	3150
AT59	59	200	1.20	5200
Az26	25	200	0.25	532
A736	35	200	0.26	1436
AZ46	45	200	0.33	2320
AZ56	55	188	0.60	4061

Table A13. Pneumatic Vibrators.

Denomination	Diameter (mm)	Frequency (Hz)	Amplitude (mm)	Centrifugal strength (N)	Assumed effective diameter (mm)
AY107	108	250	1.9	24200	
AY157	155	200	2.6	39500	
AY27	26	350	0.5		
AY37	36	317	0.6	1960	
AY47	47	300	0.6	3800	
AY57	56	300	0.8	6600	
AY67	67	283	0.9	11300	
AY77	77	267	1.2	14600	
AY87	87	265	1.8	22400	
NVV25	25	300	N.C	160	1440
NVV35	35	300	N.C	200	1924
NVV45	45	283	N.C	250	3500
NVV55	55	283	N.C	380	6050
NVV65	65	300	N.C	440	9301
NVV75	75	300	N.C	500	14851
NVV85	85	283	N.C	550	22182
NVV105	105	225	N.C	650	32460
NVV140	140	147	N.C	850	49347
NBI 30	31	200	N.C	150	990
NBI 37	38	200	N.C	380	1600
NBI 47	50	200	N.C	510	3600
NBI 57	58	200	N.C	700	5400
NBI 67	65	200	N.C	750	6600
NBI 671	65	200	N.C	850	7500

References

- [1] Francisco-José Rubio-Hernández, Rheological Behavior of Fresh Cement Pastes, *Fluids* 2018, 3, 106; doi: 10.3390/fluids3040106.
- [2] Mette Bendixen, Lars L. Iversen, Jim Best, Daniel M. Franks, Christopher R. Hackney, Edgardo M. Latrubesse, and Lucy S. Tusting, Sand, gravel, and UN Sustainable Development Goals: Conflicts, synergies, and pathways forward, *One Earth* 4, August 20, 2021.
- [3] Blaise Ngwem Bayiha, Benjamin Bahel, Fabien Kenmogne, Ulrich Nota Yemetio, Emmanuel Yamb, and Ndigui Billong, Comparative study of the effects of a natural pozzolan and an artificial pozzolan on the hydraulic properties of Portland cement mortar, *Global Journal of Engineering and Technology Advances*, 2023, 14(01), 107-119.
- [4] Lionel Lemay, Colin Lobo and Karthik Obla, Sustainable Concrete: The Role of Performance-based Specifications, Conference: Structures Congress 2013, DOI: 10.1061/9780784412848.234.
- [5] Fernando Menezes de Almeida Filho, Mounir K. El Debs and Ana Lúcia H. de Cresce El Debs, Bond-slip behavior of self-compacting concrete and vibrated concrete using pull-out and beam tests, *July 2008 Materials and Structures* 41(6): 1073-1089.
- [6] CimBéton. (1998). La vibration des bétons, Collection Technique CimBéton ed. 1998. Concrete Research, vol. 26, no. 2, pp. 283-294, 1996.
- [7] Dupuy, J. (1930)"Un excellent appareil vibreur "La table vibrante", " *Revue des matériaux de Construction et de travaux publics*, pp. 458-459.
- [8] Ho D. W. S, Sheinn A. M. M. and Tam C. T., "Rheological model for self-compacting concrete- paste rheology", *Proc. 27 th Conference on Our World in Concrete & Structures*, 29-30 August 2002, Singapore, pp 517-523. (Awarded paper for Young Concrete Researcher Award, 2002).
- [9] Martial Nde Ngnihamy, Fabien Kenmogne, André Abanda, Michel Mbessa, Jean-De-La-Croix Gnappoun, and Didier Fokwa, A Simple Benchmark to Evaluate the Influence Parameters of the Microstructure of the Masonry Wall on Capillary Water Migration Dynamic, *Advances in Civil Engineering Volume 2022*, Article ID 9292794, 12 pages. <https://doi.org/10.1155/2022/9292794>

- [10] B. A. Herki, Jamal M Khatib, Valorisation of waste expanded polystyrene in concrete using a novel recycling technique, *European Journal of Environmental and Civil engineering*, 21: 11, 1384-1402, (2017) DOI: 10.1080/19648189.2016.1170729.
- [11] Shiping Wei, Zhenglong Jiang, Hao Liu, Dongsheng Zhou, and Mauricio Sanchez-Silva, Microbiologically induced deterioration of concrete - A Review, *Braz J Microbiol.* 2013 Dec; 44(4): 1001-1007.
- [12] Willy Arnold Donda Fonchou, André Abanda, Fabien Kenmogne, Moussa Sali, Jérémie Madja Doumbaye, Partial Replacement of Cement with Waste Glass Powder in Concrete for Sustainable Waste Management: A Case Study of Concrete Incorporating Sand and Waste Glass from the Douala City of Cameroon, *American Journal of Materials Science* 2023, 13(1): 7-21.
- [13] Nicolas, R. (2004). "Analyse des impacts environnementaux des constructions en béton," in *Plaçant - Essai d'étalement au cône d'Abrams.*, (2010). Structures, vol. 41, pp. 1073-1089.
- [14] J. Spangenberg, N. Roussel, J. H. Hattel, H. Stang, J. Skocek and M. R. Geiker, Flow induced particle migration in fresh concrete: Theoretical frame, numerical simulations and experimental results on model fluids, *Cement and Concrete Research*, Volume 42, Issue 4, April 2012, Pages 633-641.
- [15] Guillaume Grampeix, Effect of internal vibration and concrete rheology on properties of reinforced concrete, *Proceedings of the 9th fib International PhD Symposium in Civil Engineering: Karlsruhe Institute of Technology (KIT)*, 22-25 July 2012, Karlsruhe, Germany.
- [16] Mary, M. (1936). *Etude de la vibration du béton*, Annales des Ponts et Chaussées ed., 1936, vol. 1-4.
- [17] Nicolas, J. (mai 2009). "Bétons Extrêmes," *Les Cahiers Techniques du Bâtiment*, no. 288, pp. 32-49.
- [18] André Abanda, Fabien Kenmogne, Ahoudou Ngamie Ndoukouo, Timothé Thierry Odi Enyegue, Martial N. Nde, and Kevin G. Ngana, Evaluating the influence of selected concrete admixtures on the physical, chemical and mechanical properties of paste and mortar samples cured under cameroonian climate conditions, *American Journal of Innovative Research and Applied Sciences*. ISSN 2429-5396 (2024).